RSC Advances

ROYAL SOCIETY
OF CHEMISTRY

www.rsc.org/advances

1   **Antibiotics detoxification from synthetic and real effluents using a novel**

2   **MTAB surfactant-montmorillonite (organoclay) sorbent**

3

4   Merry Anggraini[†], Alfin Kurniawan[†], Lu Ki Ong[†], Mario A. Martin[†], Jhy-Chern Liu[‡], Felycia

5   E. Soetaredjo[†], Nani Indraswati[†], Suryadi Ismadji[†,*]

6

7   [†] Department of Chemical Engineering, Widya Mandala Surabaya Catholic University,

8   Kalijudan 37, Surabaya 60114, Indonesia

9   [‡] Department of Chemical Engineering, National Taiwan University of Science and

10   Technology, No. 43, Sec. 4, Keelung Rd., Taipei City 106, Taiwan (R.O.C)

11

12   [*] Corresponding author: S. Ismadji, e-mail address: suryadiismadji@yahoo.com, Tel.: +62 31

13   389 1264, Fax: +62 31 389 1267

14

15

16   **Abstract**

17   The growing threats of antibiotic-resistant bacteria to public health have raised attentions to

18   properly treat the discharged pharmaceutical wastewater before entering into the surface

19   waters. In this study, adsorption was highlighted as a low cost and effective pathway to

20   remove amoxicillin and ampicillin from aqueous solutions. Montmorillonite (Na-MMT) and

21   myristyltrimethylammonium (MTA)-intercalated montmorillonite (O-MMT) were employed

22   as the adsorbing solids. Static adsorption experiments were performed at three temperatures

23   (303.15 K, 313.15 K and 323.15 K) for single antibiotic systems. The adsorption isotherm

24   curves at all temperatures exhibited a L2-type isotherm. The Freundlich and Langmuir

25   models were applied to analyze single adsorption isotherm data. The maximum sorption

26   capacity of 0.124-0.133 mmol/g for amoxicillin and 0.143-0.157 mmol/g for ampicillin was

27   estimated for O-MMT sorbent from Langmuir fitting. A modified extended-Langmuir model

28   with the inclusion of surface coverage (θ) was proposed for analysis of binary adsorption

29   isotherm data. The fitness of modified extended-Langmuir model was superior to the original

30   model. Batch adsorption tests on real pharmaceutical wastewater demonstrated the feasibility

31   of O-MMT sorbent for practical applications.

32   **Keywords:** Amoxicillin; Ampicillin; Microwave irradiation; Adsorption isotherms;

33   Extended-Langmuir model; Surface coverage

INTRODUCTION

Currently, a large group of antibiotics is available in the market and have been proven to be powerful drugs to treat various bacterial infections, from minor to life-threatening ones. Antibiotics are generally produced by or derived from microorganisms such as fungi or bacteria and they can also be chemically synthesized and particular examples are penicillins, cephalosporins, macrolides, rifamycins, sulfonamides, chloramphenicol, tetracyclines and aminoglycosides. Of particular interest are penicillin groups include amoxicillin and ampicillin. Amoxicillin is a moderate-spectrum of β-lactam antibiotics and is usually the drug of choice within penicillin groups due to its better absorptivity, following oral administration than other β-lactam antibiotics. Amoxicillin is widely used in the treatment of a number of bacterial infections include pneumonia, bronchitis, laryngitis, gonorrhea, skin and urinary tract infections.[1] Ampicillin is also a β-lactam antibiotic, part of the aminopenicillin family, which is closely related to amoxicillin in terms of spectrum and activity level.[2] Both amoxicillin and ampicillin work in a similar manner against Gram Positive and Gram Negative bacteria by interfering cell wall synthesis so that the human antibodies can penetrate and remove them.[2] In spite of its usefulness and valuable contributions in human therapy, antibiotic-resistant bacteria are the today's most pressing clinical and public health concerns that continue to grow due to abuse and overuse of antibiotics. This leads to consequent treatment complications and increased healthcare costs because the target bacteria are becoming more resistant to the exposure of therapeutic levels of an antibiotic.

The dissemination of antibiotics in natural environments (e.g., lakes and streams) may come from various sources, such as human and animal excretion, agriculture, aquaculture and livestock farming, hospital sewage sludge and diverse industrial routes.[3] The relative concentrations of antibiotics in the industrial effluents are several order of magnitude higher

59   than those released from veterinary and hospital sources.[3] Although most of pharmaceutical

60   products administered are particularly designed to have a short half-life, some antimicrobials

61   like tetracycline, erythromycin, sulfamethoxazole and penicilloyl groups are persistence and

62   poorly metabolized hence they are only partially eliminated in the sewage treatment plants.

63   The enrichment of antibiotic residues and their transformed products into receiving waters is

64   worrying as it can impact the structure and activity of microbiota, spreading of antibiotic-

65   resistant genes to pathogenic bacteria strains that can reach humans through food chains and

66   ultimately in the water reuse scenario.[4-6]

67

68   Several treatment methods have been developed so far for purification of antibiotic-bearing

69   effluents such as aerobic and anaerobic biological treatments[7,8], advanced chemical

70   oxidation[9-11], membrane separation[12], chlorination[13], photocatalysis[14-16], electro-oxidation[17],

71   and adsorption[18-21]. Amongst them, adsorption is considered as the most reliable method for

72   removal of toxic micropollutants from municipal water and wastewater. Regardless of the

73   adsorbent material and system design, adsorption process is generally simple, adaptable,

74   economically viable and highly effective across a wide range of concentrations, highlighting

75   its advantages over other technologies. The treatment of water and wastewater containing

76   antibiotics by adsorption is the key to modulating the extent of environmental occurrence,

77   transport and fate of this micropollutant.

78

79   Clays and clay minerals have found potential applications for sustaining the environment

80   because they exhibit large adsorption capacity, excellent mechanical and chemical stability,

81   cheap and readily obtained in large quantities. So, efforts toward their applications as a

82   sorbent to abate antibiotics from water and wastewater have been stimulated. Over the past

83   few years, a progressing research on the removal of antibiotics using clays or clay minerals

84   can be found in literatures.[18-21] In most, if not all, of these studies, single adsorption systems

85   are emphasized and only limited studies dedicate to investigate binary or multicomponent

86   systems. In the real pharmaceutical sewage treatment units, two or more unmetabolized

87   antibiotics may co-exist, thus it is necessary to study binary or multicomponent adsorption

88   equilibria and thermodynamics for effective design and optimization of antibiotic/clay

89   wastewater treatment systems. To fill this gap, the goals of this study are (1) to synthesize a

90   novel organoclay sorbent and (2) to evaluate the performance of pristine and as-synthesized

91   organoclay to remove amoxicillin and ampicillin from single and binary (two components)

92   aqueous systems. As far as we are aware, this is the first study demonstrating binary

93   adsorption of amoxicillin and ampicillin using pristine and myristyltrimethylammonium

94   cation-intercalated (organo) montmorillonite with special attentions to adsorption equilibria

95   and thermodynamic aspects. We propose a modification on the extended-Langmuir model by

96   introducing surface coverage for analyzing binary adsorption equilibrium data. Ultimately,

97   batch adsorption tests on real pharmaceutical wastewater are demonstrated, along with

98   regenerability evaluation of the clay sorbent.

99

100   **EXPERIMENTAL SECTION**

101   *Chemicals*

102   Antibiotics used in this study (i.e., amoxicillin trihydrate and ampicillin trihydrate) were

103   kindly provided by a local pharmaceutical industry with minimum purity of 97% and 95%,

104   respectively. The molecular structure and some specific information about these compounds

105   include their environmental persistence data[22,23] are presented in Table 1. Analytical-grade

106   chemicals include myristyltrimethylammonium bromide (MTAB) cationic surfactant (99%),

107   hydrogen peroxide solution (30%), sodium chloride (99.5%), hydrochloric acid (37%), silver

108   nitrate (99.8%) and potassium hydroxide (85%) were purchased from Sigma−Aldrich,

109   Singapore and used as-supplied. Double distilled water (DDW) was used throughout the

110   experiments.

111

112   *Preparation of adsorbent materials*

113   Montmorillonite lumps as the starting material were collected from one of mining sites

114   located at Pacitan town, East Java. After the collection, the solid was repeatedly washed with

115   tap water to remove coarse particles and water-soluble impurities. Then, the solid was

116   dispersed in dilute hydrogen peroxide solution with a solid/solution ratio of 1:10 (w/v) and

117   the suspension was aged for 2 h under mechanical stirring at 500 rpm. The solid was washed

118   with double distilled water and 0.1 N NaOH solution alternately until the pH of the washing

119   solution was near-neutral. The clay material was oven-dried at 383.15 K and stored in an

120   airtight plastic bag for further characterizations. The mineralogical analysis of clay material

121   was conducted based on the size fractionations method[24] and the results are: 72% smectite,

122   4% quartz, 12% feldspar, 8% calcite, 3% anatase and 1% others.

123

124   To enhance the monoionic nature of clay, fifty grams of clay was treated with 250 mL 1 N

125   NaCl solution (five cycles stirred at 500 rpm for an hour in each cycle) and washed until

126   negative reaction of chloride ions with silver nitrate was obtained. The resulting clay

127   (denoted as Na-MMT) was oven-dried at 373.15 K for 24 h, pulverized and screened with

128   100/120 sieves to obtain size fractions of 0.125-0.150 mm. The cation exchange capacity

129   (CEC) of Na-MMT was 74.2 meq/100 g of clay, as measured by methylene blue index

130   following ASTM C837-99 test method. The metal oxide compositions of Na-MMT were

131   analyzed using a PANalytical MiniPal QC energy dispersive X-ray fluorescence (EDXRF)

132   spectrometer and the results are shown as follows: SiO_2 of 61.28%; Al_2O_3 of 18.33%; Na_2O

133   of 2.47%, K_2O of 1.75%, MgO of 2.16%, CaO of 1.59%, MnO of 0.27%, Fe_2O_3 of 3.35%,

134   and TiO_2 of 0.08%.

135

136   The preparation procedure of organo-montmorillonite (designated as O-MMT) was described

137   as follows: 10 g Na-MMT was dispersed in 100 mL MTAB solution with a surfactant

138   concentration equivalent to 1.5 times of the CEC of clay. The suspension was aged for 1 h

139   under stirring at 500 rpm. Then, it was placed in an Inextron WDS900DSL23-2 microwave

140   oven and irradiated over 5 min at a frequency of 2.45 GHz and an output power of 500 W.

141   The resulting solid was washed with double distilled water several times until it was free

142   from bromide anions (tested by titration with 0.1 M $AgNO_3$ solution). The product was dried

143   in an air-circulating oven at 383.15 K to constant weight, pulverized and sieved. The CEC of

144   O-MMT was 14.9 meq/100 g of clay according to methylene blue adsorption index.

145

146   *Characterizations of adsorbent materials*

147   Scanning electron microscopy (SEM) was performed to probe the microtopography and

148   surface texture of the adsorbents. The scanning was conducted on a JEOL JSM-6390 field

149   emission SEM at an accelerating voltage of 20 kV. Surface characterizations were conducted

150   by physical adsorption-desorption isotherms of N_2 at 77.15 K, on a Micromeritics ASAP

151   2010 automated sorptometer. The samples were vacuum-outgassed under a flow of pure

152   helium at 10^{-3} Torr and 473.15 K for 24 h. The specific surface area, micropore volume (V_{mic})

153   and external (mesoporous) surface area (S_{ext}) was determined from the adsorption branches

154   applying the Brunauer-Emmett-Teller (BET) and *t*-plot method, respectively. The pore size

155   distribution was derived from desorption data by means of Barrett-Joyner-Halenda (BJH)

156   method. Total pore volume (V_T) was estimated from the volume of gas adsorbed at a relative

157   pressure ($p/p°$) of 0.99.

158

159 The pH of point of zero charge (pH_{pzc}) was determined by pH-drift technique following Yang

160 et al.[25] method. Briefly, a solution of 0.005 M $CaCl_2$ was boiled to remove dissolved CO_2 and

161 then cooled to room temperature. A 20 mL aliquot of the solution was poured into a series of

162 capped vials. The pH was adjusted by adding 0.5 M HCl or 0.5 M NaOH solution to a value

163 between 2 and 11. A known amount of Na-MMT or O-MMT ($\pm$ 0.05 g) was added and the

164 suspension was equilibrated for 24 h. The final pH was measured using a SevenEasy™

165 digital pH-meter (Model S20, Mettler Toledo) and plotted against the initial pH. The pH at

166 which the curve of pH_{final} versus $pH_{initial}$ crosses the line $pH_{initial} = pH_{final}$ is marked as pH_{pzc}.

167 The results are 5.82 for pH_{pzc} of Na-MMT and 7.18 for pH_{pzc} of O-MMT.

168

169 Thermal decomposition analysis was performed on a Mettler-Toledo TGA/DSC 1

170 thermogravimetric analyzer. Approximately 10 mg of the samples was spread uniformly at

171 the bottom of alumina crucible. The temperature of furnace was programmed to rise from

172 room temperature to a final temperature of 1123.15 K at 20 K/min in a dynamic high-purity

173 flowing N_2 of 100 mL/min. The elemental contents of Na-MMT and O-MMT materials were

174 determined using an automated CHNS/O elemental analyzer (Model 2400-II, PerkinElmer).

175 FT-IR analysis was carried out on a Shimadzu FTIR 8400S spectrometer using KBr disk

176 technique. The spectra data were collected by accumulating 200 scans over wavenumber

177 range of 4000-500 cm^{-1} in the transmission mode at a spectral resolution of 4 cm^{-1}. Data

178 processing includes baseline adjustment, normalization and spectral smoothing was

179 performed using IRsolution software (Version 1.21). The mineralogical compositions of the

180 solids were analyzed using a Philips PANalytical X'Pert X-ray diffractometer. The powder

181 diffractograms of the specimens were acquired at 40 kV and 30 mA in the range of 2-theta

182 angles of 2-70° with a scanning speed of 1°/min. The radiation source was Ni-filtered Cu Kα₁

183 (λ = 0.15405 nm).

184

185 *Batch adsorption experiments – single solute systems*

186 Fresh antibiotic effluents were prepared by dissolving 0.3 g amoxicillin or ampicillin into 1 L

187 deionized water to give an initial concentration of 0.80 mmol/L for amoxicillin and 0.82

188 mmol/L for ampicillin. For the adsorption equilibrium experiments, the stock effluents of

189 amoxicillin or ampicillin were poured into a series of stoppered conical flasks (each of 100

190 mL) containing Na-MMT or O-MMT with varying doses (0.1-1 g). The flasks were wrapped

191 with aluminium foil to eliminate light interference. Then, the flasks were placed in a

192 thermostated reciprocal shaker and shaken at 100 rpm for 24 h. Preliminary experiments

193 indicated that 24 h provided sufficient time to reach equilibrium. The system temperature was

194 held constant at 303.15 K, 313.15 K and 323.15 K by a built-in PID-type temperature

195 controller. After equilibration, the clay suspension was centrifuged at 3000 rpm for 10 min

196 and the supernatant was taken for analysis. The residual concentration of solute was

197 quantified by a double beam UV-Vis spectrophotometer at a detection wavelength of 252.2

198 nm for amoxicillin and 245.8 nm for ampicillin. The calibration curves were prepared from a

199 set of five standard solutions with concentration range of 50-300 mg/L. Prior to

200 spectrophotometric measurements, all supernatants were filtered through a 0.45-µm syringe

201 filter. The amount of solute adsorbed per unit mass of adsorbent at equilibrium (q_e, mmol/g)

202 was determined by the following equation:

203 $q_e = \dfrac{C_0 - C_e}{m} V$ (1)

204 where C_0 and C_e are the initial and equilibrium concentrations of solute in the liquid phase

205 (mmol/L), respectively, m is the mass of adsorbent (g) and V is the volume of solution (L).

206 For the pH adsorption edge experiments, the suspension pH was varied from 2 to 11 and

207 adjustment was made by adding 1 N HCl or 1 N KOH solutions. All adsorption runs were

208 replicated twice with averages used as the results.

209

210 *Batch adsorption experiments − binary solute systems*

211 For the binary adsorption experiments, three synthetic effluents containing amoxicillin and

212 ampicillin were prepared (Table S1 of the Supplementary Information). Adsorption isotherm

213 experiments were performed in a closed batch system by equilibrating the synthetic effluents

214 containing a known amount of O-MMT on a reciprocal shaker for 24 h at room temperature.

215 The initial pH of all effluents ranged between 6 and 7. The equilibrium concentration of

216 remaining antibiotics was determined spectrophotometrically in a multi-component

217 quantitation mode at two measurement wavelengths of 245.8 nm and 252.2 nm. Five mixed

218 samples with pure amoxicillin and ampicillin standards were made to construct the

219 calibration curve. The following mathematical formula was used to calculate the equilibrium

220 amount of solutes *i* and *j* in the adsorbed phase:

221
$$q_{e,i/j} = \frac{\left(C_{0,i/j} - C_{e,i/j}\right)}{m} \times V \tag{2}$$

222 where $q_{e,i}$ and $q_{e,j}$ are the equilibrium loading of solutes *i* and *j* in the solid phase (mmol/g), C_0

223 and C_e refer to the initial and equilibrium concentrations of solute in the solution (mmol/L),

224 *m* is the mass of O-MMT used (g) and *V* is the volume of the effluents (L).

225

226 **RESULTS AND DISCUSSION**

227 *Textural properties and surface chemistry of Na-MMT and O-MMT materials*

228 The electron micrographs of Na-MMT and O-MMT are shown in Figure 1. SEM analysis

229 confirmed that Na-MMT and O-MMT are both crystalline solids of micrometer size. The

230 lump alike morphology of Na-MMT with smooth surface characteristic is clearly seen from

231   Fig. 1a. In comparison, the SEM image of O-MMT displays the agglomerated sheet alike

232   morphological feature and surface roughness (Fig. 1b). N_2 adsorption-desorption isotherms

233   (Fig. S1 of the Supplementary Information) ascertain that both clay sorbents are highly

234   mesoporous with mixed micro- and meso-sized pores. The characteristic type H4 hysteresis

235   loop observed in the relative pressure range of 0.4-0.6 is the indication of an adsorption

236   phenomenon of gases typical for complex micro-mesoporous solids, which include

237   micropores filling, pore condensation and cavitation-induced evaporation mechanisms.[26] The

238   BET specific surface area of Na-MMT was 122.2 m^2/g and this value dramatically fell to

239   65.8 m^2/g of O-MMT. Similarly, total pore volume of Na-MMT was 0.11 cm^3/g while that of

240   O-MMT was 0.06 cm^3/g (Table S2 of the Supplementary Information). The decreased BET

241   specific surface area and pore volume revealed that some interior adsorption sites became

242   inaccessible by N_2 molecules due to the blocking of large surfactant cations within the pores.

243   The pore size distribution curves (inset Fig. S1) support N_2 adsorption-desorption results that

244   high percentage of mesopores with a diameter about 3-4 nm exist in Na-MMT and O-MMT.

245   Furthermore, a notable distribution of pore sizes outside the range of 3-4 nm was observed in

246   O-MMT, likely due to the surfactant cations loading into the interparticle pores within the

247   'house-of-cards' structure that enlarge the corresponding pore size. This is consistent with

248   other studies dealing with organoclay preparation employing long alkyl-chain cationic

249   surfactants.[27-29] Confirmation of the organification of Na-MMT was also shown from

250   elemental analysis results in the supplementary information Table S3. In this table, it can be

251   seen that O-MMT contains about 0.83 wt% N and 12.1 wt% C (the C/N ratio is 14.58) where

252   the presence of carbon and nitrogen atoms in Na-MMT is not observed. Based on the carbon

253   and nitrogen contents, it can be estimated that each gram of clay contains 0.59 mmol of

254   intercalated C14-trimethylammonium cations.

255

256   Thermal gravimetric analysis was used to examine the weight loss arising from organic

257   content and the related degradation mechanisms. The TGA curves in the supplementary

258   information Figure S2 show that the weight loss by about 7% below 150 °C corresponds to

259   the loss of surface water and water associated with Na-MMT micropore structure. Between

260   200 °C and 400 °C, about 0.0063 g H_2O/g clay was lost, which might be attributed to

261   desorption of water from the interlayer space. Irreversible dehydroxylation of the layered

262   silicate structure takes place in the temperature range of 600-700 °C. The weight change of

263   the clay could be neglected above 700 °C. The presence of organic moieties increases the

264   number of decomposition steps for organoclay. As illustrated in Fig. S2, the TGA profile of

265   O-MMT indicates four weight-loss steps: (I) the loss of water (dehydration) that occurs at

266   110 °C and ends at 150 °C; (II) decomposition of the bonded structure of organic modifier in

267   the interlayer space at 200-300 °C; (III) dehydroxylation of the silicate layers around 600 °C

268   and proceeds till around 700 °C and (IV) further decomposition of the organic surfactant at

269   720-800 °C. The thermogram pattern of bare MTAB indicates the weight loss at 110 °C

270   resulted from dehydration, followed by structural degradation that occurs at 250-400 °C.

271   Finally, the maximum decomposition takes place around 600 °C due to the incomplete

272   oxidation of the organic moieties under N_2 atmosphere.

273

274   The spectral characteristics of Na-MMT and O-MMT are displayed in the supplementary

275   information Figure S3. Several infrared absorption bands of Na-MMT were observed at

276   specific wavenumbers, which are the typical of montmorillonitic mineral: 3614 cm^{-1} of O–H

277   stretching of structural hydroxyl groups located at the surface and along the broken edges,

278   3342 cm^{-1} and 1636 cm^{-1} of stretching and bending vibrations of OH group in water

279   molecules, 1087 cm^{-1} of Si–O stretching, 936 cm^{-1} of Al–Al–OH hydroxyl-bending

280   vibration, 522 cm^{-1} of Al−O−Si bending vibration and 475 cm^{-1} of Si−O−Si bending

281   vibration. The insertion of organic modifier (MTA$^+$ cation) into the interlayer spacing gave

282   rise to symmetric and asymmetric sp^3 C−H stretching vibrations of methyl and methylene

283   groups at 2900-2800 cm^{-1} and symmetric sp^3 C−H bending vibration at 1464 cm^{-1}. It can be

284   shown that the vibrational bands correspond to Si−O stretching, Al−Al−OH bending,

285   Al−O−Si bending and Si−O−Si bending between Na-MMT and O-MMT are essentially

286   identical. This suggests that the unit-cell framework of montmorillonite mineral (tetrahedral-

287   octahedral-tetrahedral layered sheets) remains intact during microwave irradiation. On the

288   other hand, the absorption intensities of stretching and bending vibrations of hydroxyl group

289   at ~3400 cm^{-1} and ~1600 cm^{-1} dropped, which might be attributed to the removal of adsorbed

290   water molecules from the clay lattice.

291

292   X-ray diffractograms of Na-MMT and O-MMT are given in the supplementary information

293   Figure S4. Here, the XRD pattern of MMT lump was not shown due to its similar

294   characteristic to that pattern of Na-MMT. A broad (001) reflection was noted at 2-theta of

295   6.44° for MMT lump and 6.49° for Na-MMT, characterizing the basal spacing of

296   montmorillonite. This information suggested that the transformation of MMT lump to Na-

297   MMT through cation exchange did no or little alteration on the mineralogical properties of

298   clay. The occurrence of other crystalline phases such as quartz, calcite, feldspar and anatase

299   was observed in addition to montmorillonite crystal planes and basal reflections. Semi-

300   quantitative mineral analyses of MMT lump and Na-MMT based on XRD data showed that

301   these clay impurities accounted for 20-22% of total crystalline phases (the purity of smectite

302   phase was 78-80%). The intercalation of MTA$^+$ cations into the montmorillonite structure

303   leads to the expansion of basal spacing from 1.36 nm to 1.95 nm and interlayer spacing from

304   0.39 nm to 0.98 nm. The interlayer spacing was determined by subtracting the measured

305   basal spacing with the unit-cell thickness of a single tetrahedral-octahedral-tetrahedral

306   layered sheet of montmorillonite, which is 0.97 nm.[30] The structural conformation of the

307   surfactant in the interlayer spacing can be interpreted by considering the magnitude of

308   increased basal spacing and the molecular structure of intercalated surfactant cations (the

309   thickness of polar 'head' and apolar 'tail'). The loading of MTA^+ cation, a single C14 alkyl

310   chain trimethylammonium surfactant with a concentration of 1.5 times of the CEC would

311   result in the pseudotrilayer conformation; that is the alkyl chain of surfactant is packed in

312   parallel to the plane of silicate tetrahedral sheets with interlocked-chains array.[27,31] The

313   equivalence exchange between Na^+ and MTA^+ cations also renders the clay surface to be

314   organophilic, which is suitable to sorb organic compounds such as antibiotics.

315

316   *Effects of solution pH on the adsorptive removal of amoxicillin and ampicillin*

317   The pH is a crucial factor both towards the surface charge density of adsorbent and the ionic

318   speciation of adsorbate in the liquid phase, which determines the effectiveness of a sorption

319   process. The presence of acid (carboxylic) and base (amino) surface functional groups within

320   amoxicillin and ampicillin structure contributes to the amphoteric nature of these drugs, in

321   which these groups are ionisable following the pH changes. As shown in Table 1, amoxicillin

322   has three acid dissociation constants of 2.4 (pK_{a1} of carboxylic), 7.4 (pK_{a2} of amine) and 9.6

323   (pK_{a3} of phenol) while for ampicillin, the pK_a values are 2.7 (carboxylic) and 7.3 (amine).[14]

324   Accordingly, amoxicillin species are mainly as a cation in the acidic solution (pH < 2.4), a

325   zwitterion between pH 2.4 and 7.4 and an anion in the alkaline solution (pH > 7.4). Similarly,

326   ampicillin exists predominantly in cationic, zwitterionic and anionic forms at pH < 2.7, 2.7 <

327   pH < 7.3 and pH > 7.3, respectively (see Fig. S5 of the Supplementary Information). The

328   distribution diagrams showing the percentage of amoxicillin and ampicillin species at room

329 temperature under different solution pHs was presented in the supplementary information

330 Figure S6.

331

332 The influence of pH on the adsorbed amount of amoxicillin and ampicillin in single systems

333 is given in Figure 2. In this figure, the increasing amount of amoxicillin or ampicillin

334 adsorbed by Na-MMT was seen with the increase of pH from 2 to 7 and then a progressive

335 decrease on the removal percentage was encountered at pH above 7. Similar observation was

336 reported by Moussavi et al. for the removal of amoxicillin from water using NH_4Cl-induced

337 activated carbon.[32] The limited uptake at low pH, particularly below $p\mathrm{K}_{a1}$ of amoxicillin or

338 ampicillin was due to net repulsion between positively charged edge hydroxyl surfaces of

339 montmorillonite crystallites (silanol and aluminol sites) and the cationic adsorbate molecules.

340 From the speciation diagrams in Fig. S5, it can be shown that at low pH range (pH 2-3), the

341 cationic amoxicillin and ampicillin accounted for 84% and 86% of total species in the

342 solution, respectively. The removal processes of amoxicillin (~24%) and ampicillin (~27%)

343 could still take place in the acidic environment due to the dipole-induced interaction between

344 protonated amine group and the Si-tetrahedral basal oxygen surface in addition to ion

345 exchange between Na^+ interlayer cations and protonated amoxicillin or ampicillin. The latter

346 phenomenon (cation exchange) has been verified to be the sorption controlling mechanism at

347 low pH in the studies conducted by Jiang et al.[33] and Wang et al.[34] for the removal of

348 ciprofloxacin using layered manganese oxide and Ca-montmorillonite, respectively.

349

350 With the increase of pH approaching $p\mathrm{K}_{a2}$ of the adsorbate, the ratio of zwitterion to cation

351 increases gradually for both antibiotics and this leads to the increase of removal percentage,

352 reaching the highest level of 63.5% for amoxicillin and 65.2% for ampicillin at near-neutral

353 pH. Under this condition, the protonated amine in amoxicillin or ampicillin structure might

354   play important for the enhanced removal process by forming electric force that attracts this

355   cationic group to deprotonated aluminol (Al−O⁻) or silanol (Si−O⁻) edge sites. Furthermore,

356   the concentration of H^+ ions that compete with NH_3^+ group for the basal oxygen surfaces

357   diminished at elevated pH, facilitating the sorption process. The sorption of amoxicillin or

358   ampicillin under alkaline environment is unfavorable since both antibiotics exist as an anion

359   (attributed to the presence of conjugate bases of carboxylic acid and phenol groups) thus

360   electrostatic repulsive force dominates. Such phenomenon was confirmed from a gradual

361   decline on the removal percentage from 63.5% to 18.7% for amoxicillin and 65.2% to 20.3%

362   for ampicillin as the pH rose from 7 to 11.

363

364   For the adsorption of amoxicillin or ampicillin using O-MMT, higher removal percentage

365   was observed across the pH range studied, indicating that O-MMT has superior adsorption

366   capacity. In the acidic solution, about 31-61% of amoxicillin and 33-62% of ampicillin was

367   removed while the removal efficiency in highly alkaline environments (pH 10-11) ranged

368   between 27% and 41% for amoxicillin and 31-43% for ampicillin. The highest removal

369   percentage was obtained at pH around 7, corresponding to 77.8% removal for amoxicillin and

370   81.3% removal for ampicillin. It can be implied that higher adsorptive removal of O-MMT

371   was mainly attributed to the exchange of interlayer Na^+ cation with MTA^+ cation, which

372   provides beneficial features to the sorption process. Aside from expanding the interlayer and

373   basal spacing, the intercalation of MTA^+ cation would expose additional charge-bearing sites

374   for the binding of incoming amoxicillin or ampicillin molecules. The intercalated MTA^+

375   cation would interact hydrophobically with amoxicillin or ampicillin through intermolecular

376   attraction forces, possibly van der Waals force or permanent dipole-dipole interaction

377   between positively charged nitrogen atom located at the 'head' of MTA^+ cation and

378   negatively charged carboxylate anion (RCOO⁻) in amoxicillin or ampicillin structure. The

379   forces of electrostatic attraction acting between carboxylate anionic groups and positively

380   charged clay' edge sites might also take place. Furthermore, the hydrophobic alkyl chain of

381   the intercalated surfactant played important role by serving as a sorption domain for the

382   allocation of organic (antibiotic) molecules.[35-37] Thus, it can be argued that the intercalated

383   surfactant cation in the clay' interlayer spacing has a crucial influence by forming organic

384   partition phases with quite different affinities toward the organic groups. Ultimately, there

385   was no linear relation between the surface properties and adsorption capacity as O-MMT

386   sorbent exhibited higher sorption capacity although its specific surface area and pore volume

387   were lower compared to the original material.

388

389   *Modeling adsorption isotherm data for single antibiotic systems*

390   The so-called adsorption isotherm is vital information describing the equilibrium distribution

391   of solute adsorbed on a solid surface to that of in the liquid with which it is in contact at a

392   given temperature. The single component adsorption isotherms of amoxicillin and ampicillin

393   were analyzed by Freundlich and Langmuir models. The Freundlich model, which originally

394   developed in 1909 for expressing the isothermal variation of a quantity of gas adsorbed by

395   unit mass of adsorbent with pressure, has an empirical mathematical form as follows[38]:

396    $$q_e = K_F \times C_e^{1/n} \tag{3}$$

397   where K_F is the Freundlich constant related to the adsorption affinity $[(mg/g).(L/mg)^{1/n}$ or

398    $(mmol/g).(L/mmol)^{1/n}]$ and n is a dimensionless intensity factor characterizing the surface

399   heterogeneity degree. Generally, the value of constant n is greater than unity and the

400   adsorption favorability can be evaluated based on the following n values: favorable (2-10),

401   moderately difficult (1-2) and poor (< 1).[39]

402

403   Langmuir model is perhaps the simplest and most useful semi-empirical model for

404   interpreting various physical and chemical adsorption phenomena in gas- and liquid-phase

405   systems as well as many real sorption processes. Langmuir (1918) postulated his isotherm

406   based on the kinetic principle of adsorption of gases on the plane surfaces of ideal solids.[40]

407   The mathematical expression of Langmuir isotherm is equated by the following formula:

408   $$q_e = q_m \frac{K_L C_e}{1 + K_L C_e} \tag{4}$$

409   where q_m is the Langmuir constant of maximum sorption capacity when the solid is covered

410   with a monolayer (mg/g or mmol/g), also denotes a practical limiting sorption capacity and

411   assists in the comparison of adsorption performance and K_L is the adsorption affinity constant

412   (L/mg or L/mmol). The essential features of Langmuir isotherm can be expressed in terms of

413   equilibrium parameter R_L, with classifications of the adsorption nature: favorable − convex

414   isotherms ($0 < R_L < 1$), unfavorable − concave isotherms ($R_L > 1$), linear ($R_L = 1$) or highly

415   favorable/non-reversible ($R_L = 0$). The R_L value can be calculated using a formula proposed

416   by Weber and Chakravorti[41]:

417   $$R_L = \frac{1}{1 + K_L C_0} \tag{5}$$

418   where C_0 is the initial solute concentration in the liquid phase, which is 0.80 mmol/L for

419   amoxicillin and 0.82 mmol/L for ampicillin.

420

421   The correlations of adsorption equilibrium data were performed by nonlinear regression

422   fitting using SigmaPlot software (Version 12.3, Systat Software Inc.). Figure 3 displays the

423   fitting comparison between Freundlich and Langmuir models against single adsorption

424   equilibrium data of amoxicillin and ampicillin. The values of the fitted isotherm parameters

425   are listed in Table 2. At a glance, Langmuir isotherm describes experimental data better than

426   Freundlich isotherm. The favorability of Langmuir model also visually confirmed from the

427   isotherm curves that exhibit a convex character. According to system of classification of

428   solution adsorption isotherms suggested by Giles and colleagues[42], the isotherm curves at all

429   temperatures belong to a L2-type, which the indicative of solute adsorbed flat on the surface.

430   Similar isotherm type was found for the immobilization of tetracycline on kaolinite surface[18]

431   and adsorption of an antihistamine medicine (chlorpheniramine) using Ca-montmorillonite[21]

432   and activated charcoal[43].

433

434   Considering the adsorption affinity, this parameter can rise or fall with temperature change,

435   depending on whether physisorption or chemisorption that dominates in the sorption system.

436   In this study where chemisorption controls the adsorption of amoxicillin and ampicillin, the

437   adsorption affinity should be higher with increasing temperature because higher temperature

438   hastens the movement of solute molecules in the liquid phase to be bound on the surface.

439   Both Freundlich and Langmuir isotherms clarify this behavior, as shown in Table 2. Higher

440   affinity of solute molecules to O-MMT surface is expected because the sorbent possesses

441   organophilic surface stemming from the substitution of MTA^+ cation in place of interlayer

442   Na^+ cation. In terms of adsorptivity, ampicillin was preferentially adsorbed to the surface

443   rather than amoxicillin.

444

445   The next examination is on the parameter q_m of Langmuir model, which the indicative of

446   maximum monolayer capacity of a particular sorbent. With the increase of temperature from

447   303.15 K to 323.15 K, the maximum monolayer capacity rose from 0.079 mmol/g to 0.090

448   mmol/g for Na-MMT and from 0.143 mmol/g to 0.157 mmol/g for O-MMT if ampicillin was

449   considered as the solute. The increasing maximum monolayer capacity accompanying

450   temperature rise revealed that chemisorption was the controlling phenomenon. The remaining

451   analysis is on the parameter n of Freundlich model, which is a characteristic constant for the

452   surface heterogeneity degree. It can be seen that there is no clear correlation between this

453   parameter and temperature, as in the sorption systems of amoxicillin/Na-MMT and

454   amoxicillin/O-MMT, the values of n decrease with temperature increase while in the

455   ampicillin/O-MMT system, an opposite trend is obtained. Even, a fluctuating value of n with

456   temperature was observed in the ampicillin/Na-MMT system. It should also be noted that the

457   magnitude of constant n should be higher for the adsorption on the O-MMT surface. Again,

458   the Freundlich isotherm cannot capture this well. Therefore, it can be concluded that

459   Langmuir isotherm outperforms Freundlich isotherm in describing adsorption equilibria data.

460   In addition, the calculated R_L values all confirmed the favorable nature of adsorption process

461   across the studied temperatures.

462

463   The adsorption capacity of O-MMT was compared with other adsorbents to evaluate its

464   application as a viable alternative to treat amoxicillin and ampicillin from water and

465   wastewater. Based on the Langmuir analysis, the maximum adsorption capacity of O-MMT

466   was estimated to be 0.124-0.133 mmol/g (45.3-48.6 mg/g) for amoxicillin and 0.143-0.157

467   mmol/g (49.9-54.9 mg/g) for ampicillin. A number of studies had used activated carbons as

468   the primary adsorbent to remove various antibiotics. Ding and co-workers[44] prepared the

469   sludge-derived activated carbons to remove a mixture of 11 antibiotics include amoxicillin

470   from diluted water solutions. The estimated total adsorption capacity of 80-300 mg/g was

471   obtained from the Langmuir-Freundlich prediction. Similar adsorption capacity of bare and

472   NH_4Cl-induced activated carbons (261.8 vs. 438.6 mg/g) was reported by Moussavi et al.[32]

473   for batch adsorption of amoxicillin. Although the synthesized O-MMT exhibited lower

474   uptake capacity than carbon-based materials, the preparation method of the organoclay is

475   simpler and less energy- and time-consuming compared to chemical or thermal activation

476   pathways to synthesize the carbons. Furthermore, the montmorillonite lump used to prepare

477   the organoclay is a cheap and easily available material in large quantity. The application of

478   organo-bentonite to remove amoxicillin had been investigated by Zha and colleagues[45].

479   However, lower adsorption capacity of the organobentonite (27.85-30.12 mg/g at 303.15 K

480   and 313.15 K) was obtained compared to the values reported in this study. The O-MMT

481   sorbent also showed superior adsorption capacity than chitosan beads[46] (45.3 vs. 8.71 mg/g at

482   pH 6.5) for batch amoxicillin removal.

483

484   *Modeling adsorption isotherm data for binary antibiotic systems*

485   Multicomponent adsorption depends on the number of solutes competing for the sorption

486   sites, their speciation, concentrations, residence time, etc., which all contribute to the

487   interference and competition phenomena in the solution and at the solid/solution interface.[47]

488   Often, most of available empirical or semi-empirical models lack of theoretical basis and they

489   may not be able to accurately analyze the system behavior over the entire range of

490   measurements. Notwithstanding the most realistic model so-called the ideal adsorption

491   solution theory (IAST) and its modifications, such as fast-IAS and real adsorption solution

492   theory have found reasonable success to correlate multicomponent adsorption equilibria data,

493   the complex algorithm for the model solution involving numerical integration at each step of

494   iteration procedure requires the use of advanced computer resources. On the other hand,

495   extended-Langmuir is a simple model with adequate thermodynamic basis and useful insights

496   for analyzing multicomponent adsorption equilibria. To describe the equilibrium competitive

497   adsorption in the multicomponent systems, Langmuir model for pure component adsorption

498   equilibria can be easily extended to the following formulation:

499    $$q_{e,i} = \frac{q_{m,i} \cdot K_{L,i} \cdot C_{e,i}}{1 + \sum_{i=1}^{N} K_{L,i} \cdot C_{e,i}}$$ (6)

500   where i is the number of components, $q_{m,i}$ and $q_{e,i}$ are the maximum adsorbed amount of each

501   component (mmol/g) and the adsorbed amount of each component per mass of adsorbent at

502   equilibrium concentration $C_{e,i}$ and $K_{L,i}$ is the individual adsorption affinity constant of each

503   component (L/mmol). For a liquid phase system consisting of two components, one can use

504   the extended-Langmuir equation in the form:

505   $$q_{e,1} = \frac{q_{m,1} \cdot K_{L,1} \cdot C_{e,1}}{1 + K_{L,1} \cdot C_{e,1} + K_{L,2} \cdot C_{e,2}} \tag{7}$$

506   $$q_{e,2} = \frac{q_{m,2} \cdot K_{L,2} \cdot C_{e,2}}{1 + K_{L,1} \cdot C_{e,1} + K_{L,2} \cdot C_{e,2}} \tag{8}$$

507   The success of the extended-Langmuir model in analyzing binary adsorption equilibrium data

508   has been reported in several studies.[47-49] The validity of the model was justified based on the

509   simple error minimization between predicted and measured q_e values. The predicted q_e values

510   for each component can be calculated from Eq. (7) and Eq. (8) by introducing the fitted

511   parameters q_m and K_L belonging to single adsorption data. Such approach, however, does not

512   fit for correlating binary adsorption data because adsorption in the binary system involves

513   interference and competition between solutes in the solution and on the active surface sites;

514   both these characteristics are negated in the single adsorption system. Therefore, to improve

515   the accuracy of predictions and theoretical sound of the extended-Langmuir model, we

516   propose a modification to each parameter above by addressing competitive adsorption

517   behavior.

518

519   In the binary system, the active sorption sites are accommodated by two solutes with a

520   specific surface coverage. Therefore, the maximum sorption capacity should be the sum of

521   fraction of surface covered by each solute multiplied by its maximum sorption capacity or

522   can be expressed as follows:

523 $q_{m,bin} = q_{m,1\,(singl)} \cdot \theta_1 + q_{m,2\,(singl)} \cdot \theta_2$ (9)

524 where θ_1 and θ_2 are the fractional surface coverage of solute 1 and 2, respectively. Here, we

525 argue that total monolayer surface coverage by both solutes should not exceed unity,

526 considering that some surface sites are inactive for adsorption. The parameter K_L measures

527 how strong the solute molecules are attracted to the surface. The higher the affinity, the more

528 solute molecules are adsorbed on the surface. Since the solute species compete each other,

529 their affinities to the surface should be weaker compared to that of single adsorption system.

530 Accordingly, the use of parameter K_L from single adsorption data is not valid and a simple

531 theoretical treatment to this parameter is given as follows:

532 $K_{L,1\,(bin)} = K_{L,1\,(singl)} \left(1 - \theta_2 \middle/ \theta_1 + \theta_2 \right)$ (10)

533 $K_{L,2\,(bin)} = K_{L,2\,(singl)} \left(1 - \theta_1 \middle/ \theta_1 + \theta_2 \right)$ (11)

534 In Eq. (10) and Eq. (11), the competitive adsorption between solutes is expressed as a ratio of

535 fraction of surface covered by one solute to that of total surface coverage by both solutes.

536 Introducing Eq. (10) and Eq. (11) into Eq. (7) and Eq. (8) gives the following equations:

537 $q_{e,1\,(bin)} = \dfrac{\left(q_{m,1\,(singl)} \cdot \theta_1 + q_{m,2\,(singl)} \cdot \theta_2 \right) \cdot K_{L,1\,(singl)} \left(1 - \theta_2 \middle/ \theta_1 + \theta_2 \right) \cdot C_{e,1\,(bin)}}{1 + K_{L,1\,(singl)} \left(1 - \theta_2 \middle/ \theta_1 + \theta_2 \right) \cdot C_{e,1\,(bin)} + K_{L,2\,(singl)} \left(1 - \theta_1 \middle/ \theta_1 + \theta_2 \right) \cdot C_{e,2\,(bin)}}$ (12)

538 $q_{e,2\,(bin)} = \dfrac{\left(q_{m,1\,(singl)} \cdot \theta_1 + q_{m,2\,(singl)} \cdot \theta_2 \right) \cdot K_{L,2\,(singl)} \left(1 - \theta_1 \middle/ \theta_1 + \theta_2 \right) \cdot C_{e,2\,(bin)}}{1 + K_{L,1\,(singl)} \left(1 - \theta_2 \middle/ \theta_1 + \theta_2 \right) \cdot C_{e,1\,(bin)} + K_{L,2\,(singl)} \left(1 - \theta_1 \middle/ \theta_1 + \theta_2 \right) \cdot C_{e,2\,(bin)}}$ (13)

539 Eq. (12) and Eq. (13) are both called as the modified extended-Langmuir model. Here, θ_1 and

540 θ_2 were treated as fitting parameters with the following constraints: $\theta_1 > 0$, $\theta_2 > 0$ and $\theta_1 + \theta_2$

541 < 1. The proposed model was fitted to experimental data by performing computer-aided

542   nonlinear regression fitting. The accuracy of predictions was assessed from the coefficient of

543   determination (R^2) values obtained from the computational results.

544

545   The binary adsorption equilibrium data are obtained by conducting adsorption experiments at

546   303.15 K and near-neutral pH with O-MMT as the sorbent and mixtures of amoxicillin and

547   ampicillin as the waste effluents. Here, O-MMT was employed as the sorbent due to its

548   superior adsorption capacity compared to Na-MMT. Also, the choice of conducting binary

549   adsorption experiments at pH range of 6-7 was based on the single adsorption results in

550   which at this pH range, the highest removal of amoxicillin and ampicillin took place. Figure 4

551   shows the correlation results of binary adsorption equilibrium data fitted with the modified

552   extended-Langmuir model (represented as wire-mesh plot). The values of θ_1 and θ_2 obtained

553   from the model fitting are given in Table 3. From Figure 4, it can be seen that the modified

554   extended-Langmuir model can correlate binary adsorption data adequately. In comparison,

555   the fitness of original extended-Langmuir model to the experimental data is given in the

556   supplementary information Figure S7. Noticeably, the modified extended-Langmuir model

557   gave better representation than the original model, suggesting that the inclusion of fractional

558   surface coverage may improve the accuracy of predictions and assist in interpreting the

559   adsorption behavior in binary system. The fraction of active sorption sites covered by either

560   amoxicillin or ampicillin decreases as the concentration of the opposite adsorbate in the

561   mixture increased. For example, the fraction of adsorption sites covered by amoxicillin for

562   effluent A (75 wt.% amoxicillin + 25 wt.% ampicillin) was 0.639 and this value decreased to

563   0.437 and 0.263 with increasing ampicillin concentration to 50 wt.% and 75 wt.%,

564   respectively. Likewise, the ampicillin loading on the surface of O-MMT increased with

565   decreasing concentration of amoxicillin in the mixture. One can also notice that total

566   monolayer coverage on the surface in all systems is similar, typically about 0.89 (expressed

567   as a fractional quantity). This supports our previous argument that some of the surface sites

568   are unavailable for the sorption, likely due to the surfactant blockade and to consider that the

569   sorbent has a void fraction. With regard to adsorptivity, both amoxicillin and ampicillin are

570   less likely adsorbed on the surface due to competition effect. Consequently, fewer amounts of

571   amoxicillin (44.8%) and ampicillin (48.3%) were removed from a binary mixture (effluent B)

572   compared to single solute systems for near-neutral pH adsorption. To this end, the modified

573   extended-Langmuir model will turn back into the original Langmuir model if only one solute

574   component is considered in the sorption system (θ_2 and $C_{e,2}$ are zero in Eq. (12) and θ_1 and

575    $C_{e,1}$ are zero in Eq. (13)).

576

577   *Adsorption thermodynamic*

578   Adsorption thermodynamic relates the equilibrium of adsorption to those properties which

579   cannot be directly measured from the experiment, such as activation energy (E_a, kJ/mol), the

580   Gibb's free energy change ($\Delta G°$, kJ/mol), standard enthalpy change ($\Delta H°$, kJ/mol), standard

581   entropy change ($\Delta S°$, kJ/mol.K) and isosteric heat of adsorption (ΔH_x, kJ/mol). The Gibb's

582   free energy change is an important criterion for spontaneity of a chemical process and it can

583   be related to adsorption equilibrium constant by the following reaction isotherm:

584    $$\Delta G^0 = -RT \ln K_D \tag{14}$$

585   where R is the ideal gas constant (8.314 J/mol.K), T is the temperature (K) and K_D is the

586   linear sorption distribution coefficient, defined as a ratio between the equilibrium surface

587   concentration of adsorbed solute and the equilibrium solute concentration in the liquid phase.

588   The value of K_D is determined by plotting a straight line of ln (q_e/C_e) versus C_e and

589   extrapolating to zero C_e according to Khan and Singh[50]. The variation of thermodynamic

590   equilibrium constant with temperature can be expressed in terms of standard enthalpy change

591   and standard entropy change by the classical van't Hoff formula:

592     $$\ln K_D = \frac{\Delta S^0}{R} - \frac{\Delta H^0}{RT}$$ (15)

593   A plot of natural logarithm of the thermodynamic equilibrium constant, $\ln K_D$ versus the

594   reciprocal temperature, $1/T$ (Fig. 5) will be linear with the slope and y-intersection point

595   giving the values of $\Delta H°$ and $\Delta S°$, respectively.

596

597   Table 4 summarizes the values of thermodynamic parameters for single adsorption of

598   amoxicillin and ampicillin. The free energy change of adsorption decreased with an increase

599   in temperature and this suggests that higher temperature makes the sorption process easier.

600   The negative values of $\Delta G°$ confirm that adsorption is thermodynamically feasible and

601   spontaneous with high preference of solutes to the surface. In this case, the adsorption of

602   amoxicillin and ampicillin on O-MMT is more likely to take place at a given temperature, as

603   reflected from the magnitude of $\Delta G°$ values. The values of $\Delta H°$ and $\Delta S°$ are 43.8 kJ/mol and

604   162.8 J/mol.K for amoxicillin/Na-MMT system and 45.3 kJ/mol and 178.4 J/mol.K for

605   ampicillin/Na-MMT system. The positive sign of $\Delta H°$ is an indication of the endothermicity

606   of adsorption and suggests the possibility of strong binding between adsorbate and adsorbent.

607   Furthermore, the magnitude of $\Delta H°$ values may give an idea whether the adsorption belongs

608   to physisorption (2.1-20.9 kJ/mol) or chemisorption (80-200 kJ/mol). As shown in Table 4, it

609   seems that the adsorption of amoxicillin and ampicillin on Na-MMT or O-MMT can be

610   attributed to the combination of physisorption and chemisorption rather than a pure physical

611   or chemical adsorption.

612

613   The thermodynamic quantity $\Delta S°$ is defined as a measure of randomness in the system. The

614   positive value of $\Delta S°$ reflects high affinity of solute to the sorption sites, also the increased

615   randomness at the solid/solution interface during adsorption process. Some significant

26

616 changes in the internal structure of adsorbate and adsorbent may cause the system to gain

617 extra translational and rotational entropies, such as from the displacement of adsorbed water

618 by the adsorbate, interlayer cation exchange between Na^+ and MTA^+ or the partitioning of

619 adsorbate species in the hydrophobic alkyl chain of the intercalated surfactant. Furthermore,

620 the positive value of $\Delta S°$ revealed a strong confinement of solute in the solid phase. Since

621 binary adsorption experiments in this study were conducted at single temperature (303.15 K),

622 it is not possible to analyze thermodynamic behavior of the process. However, one can

623 predict it theoretically, for instance the values of free energy change of adsorption should be

624 less negative because adsorption is less energetically favorable. Also, the magnitude of the

625 entropy change might be greater due to increased disorder in the system as a result of

626 competitive adsorption between the adsorbed components.

627

628 *Batch adsorption tests using real pharmaceutical wastewater and regenerability evaluation*

629 In order to test the feasibility of O-MMT adsorbent for real sorption application, batch

630 adsorption experiments using real pharmaceutical wastewater were conducted at 303.15 K for

631 24 h. The adsorbent dose was fixed at 10 g/L. The wastewater was randomly collected from

632 five sampling points from a wastewater treatment plant of local pharmaceutical and health

633 care products manufacturer at Sidoarjo city, East Java. Prior to adsorption, the collected

634 samples were vacuum-filtered with a Buchner funnel to remove coarse particles. The initial

635 pH of the wastewater ranged between 5.5 and 6. Amoxicillin and ampicillin were detected as

636 two major constituents with initial concentrations of 0.16 and 0.11 mmol/L, respectively.

637 Other antibiotics, such as ciprofloxacin, chloramphenicol and cefotaxime were also detected

638 in trace levels (Table S4 in the Supplementary Information).

639

640   Solution of 0.1 M CaCl$_2$ was used as the desorbing agent. Desorption experiments were

641   carried out by mixing antibiotics-loaded O-MMT sorbent with CaCl$_2$ (solution to solid ratio

642   of 100) and the mixture was allowed to stand for 24 h under shaking at room temperature.

643   The removal percentages of each antibiotic as a function of regeneration cycle are displayed

644   in Figure 6. The highest removal percentage was observed for amoxicillin, followed by

645   ampicillin, chloramphenicol, ciprofloxacin and cefotaxime with total removal percentage of

646   68.2%. A gradual decrease in the removal percentage of each antibiotic was noticed as the

647   regeneration cycles progressed; likely due to the inability of desorbing solution to completely

648   detach bound antibiotics from the organoclay surface. Similar observation was obtained by

649   Wu et al.[51] for desorption studies of ciprofloxacin from kaolinite and montmorillonite clays.

650   By the end of the fifth cycle, total removal percentage of all antibiotics by O-MMT was

651   49.5%. These results show that O-MMT is a promising sorbent for economical and effective

652   treatment of real effluents containing antibiotic compounds. Furthermore, O-MMT sorbent

653   possesses good adsorptive retention since total removal percentage was about 50% even after

654   five successive adsorption-desorption cycles. Desorption of antibiotics from the organoclay

655   surface might be due to ligand-promoted dissolution of metal-antibiotic surface complexes

656   between Ca^{2+} and the zwitterionized antibiotics through the involvement of carboxylic

657   (−COO$^-$) groups[51,52]. FT-IR spectroscopy study of O-MMT sorbent after desorption by CaCl$_2$

658   solution (see Fig. S2 in the Supporting Information) supported this argument in which the

659   intensities of absorption peaks associated with C=O stretching of carboxylic group at ~1700

660   cm^{-1} and N−H stretching and bending vibrations of amine group at ~3400 cm^{-1} and ~1600

661   cm^{-1} diminished. In addition, the stretching peaks correspond to sp^3 C−H bond in CH$_3$ and

662   CH$_2$ groups at 2900-2800 cm^{-1} remain unaltered after Ca^{2+} desorption, indicating that cation

663   exchange between MTA$^+$ in the interlayer spacing and Ca^{2+} was not feasible to take place,

664   due to the latter cation possesses lower affinity than the former toward the clay surface.

665

CONCLUSIONS

666

Organo-montmorillonite (O-MMT) with high adsorption capacity and organophilic surface

667

has been succesfully prepared by microwave-assisted irradiation of aqueous suspension

668

containing Na-montmorillonite (Na-MMT) and MTAB cationic surfactant. The synthesized

669

O-MMT showed potential applications for detoxifying amoxicillin and ampicillin in single

670

and binary systems. Analysis of adsorption equilibrium data for single antibiotic systems

671

revealed that Langmuir model outperformed Freundlich model. The proposed extended-

672

Langmuir model with the inclusion of surface coverage was superior to original model in

673

representing binary adsorption equilibrium data. The proposed model can also adequately

674

capture theoretical insights of binary sorption behavior. Thermodynamically, the adsorption

675

of amoxicillin and ampicillin on Na-MMT/O-MMT was energetically favorable/spontaneous

676

($\Delta G° < 0$) and endothermic ($\Delta H° > 0$) with high preference of adsorbed solutes toward the

677

surface ($\Delta S° > 0$). The regeneration study revealed the feasibility of O-MMT sorbent to be

678

efficiently reused for five cycles of adsorption-desorption in handling real pharmaceutical

679

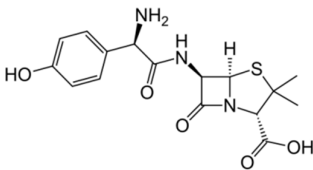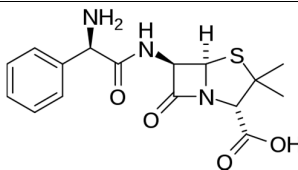wastewater containing multiple antibiotic compounds.

680

681

REFERENCES

682

(1)   R. N. Brogden, A. Carmine, R. C. Heel, P. A. Morley, T. M. Speight and G. S. Avery,

683

Drugs, 1981, **22**, 337-362.

684

(2)   J. P. Hou and J. W. Poole, *J. Pharm. Sci.*, 1971, **60**, 503-532.

685

(3)   H. Schmitt and J. Rombke, in *Pharmaceuticals in the Environment: Sources, Fate,*

686

Effects and Risks, ed. K. Kummerer, Springer Berlin Heidelberg, Berlin, 2008, pp. 285-

687

303.

688

(4)   M. V. Walter and J. W. Vennes, *Appl. Environ. Microbiol.*, 1985, **50**, 930-933.

689

690   (5)   L. Guardabassi, D. M. A. Lo Fo Wong and A. Dalsgaard, *Water Res.*, 2002, **36**, 1955-

691   1964.

692   (6)   M. L. Richardson and J. M. Bowron, *J. Pharm. Pharmacol.*, 1985, **37**, 1-12.

693   (7)   T. Coskun, H. A. Kabuk, K. B. Varinca, E. Debik, I. Durak and C. Kavurt, *Bioresour.*

694   *Technol.*, 2012, **121**, 31-35.

695   (8)   S. Larcher and V. Yargeau, *Appl. Microbiol. Biotechnol.*, 2012, **96**, 309-318.

696   (9)   R. Andreozzi, M. Canterino, R. Marotta and N. Paxeus, *J. Hazard. Mater.*, 2005, **122**,

697   243-250.

698   (10) I. A. Balcioglu and M. Otker, *Chemosphere*, 2003, **50**, 85-95.

699   (11) K. A. Rickman and S. P. Mezyk, *Chemosphere*, 2010, **81**, 359-365.

700   (12) S. Z. Li, X. Y. Li and D. Z. Wang, *Sep. Purif. Technol.*, 2004, **34**, 109-114.

701   (13) Z. Qiang, J. J. Macauley, M. R. Mormile, R. Surampalli and C. D. Adams, *J. Agric.*

702   *Food Chem.*, 2006, **54**, 8144-8154.

703   (14) E. S. Elmolla and M. Chaudhuri, *J. Hazard. Mater.*, 2010, **173**, 445-449.

704   (15) E. S. Elmolla and M. Chaudhuri, *Desalination*, 2011, **272**, 218-224.

705   (16) X. Xiao, R. P. Hu, C. Liu, C. L. Xing, X. X. Zuo, J. M. Nan and L. S. Wang, *Chem.*

706   *Eng. J.*, 2013, **225**, 790-797.

707   (17) M. Miyata, I. Ihara, G. Yoshid, K. Toyod and K. Umetsu, *Water Sci. Technol.*, 2011,

708   **63**, 456-461.

709   (18) Z. H. Li, L. Schulz, C. Ackley and N. Fenske, *J. Colloid Interface Sci.*, 2010, **351**, 254-

710   260.

711   (19) W. Yan, J. F. Zhang and C. Y. Jing, *J. Colloid Interface Sci.*, 2013, **390**, 196-203.

712   (20) N. Liu, M. x. Wang, M. m. Liu, F. Liu, L. P. Weng, L. K. Koopal and W. f. Tan, *J.*

713   *Hazard. Mater.*, 2012, **225-226**, 28-35.

714   (21) Z. H. Li, P. H. Chang, J. S. Jean, W. T. Jiang and H. L. Hong, *Colloids Surf. A*, 2011,

715   **385**, 213-218.

716   (22) S. M. Mitchell, J. L. Ullman, A. L. Teel and R. J. Watts, *Sci. Total Environ.*, 2014, **466-**

717   **467**, 547-555.

718   (23) H. Xu, W. J. Cooper, J. Jung and W. Song, *Water Res.*, 2011, **45**, 632-638.

719   (24) S. J. Chipera, G. D. Guthrie and D. L. Bish, *Rev. Mineral. Geochem.*, 1993, **28**, 235-

720   249.

721   (25) Y. Yang, Y. Chun, G. Y. Sheng and M. S. Huang, *Langmuir*, 2004, **20**, 6736-6741.

722   (26) P. L. Ravikovitch and A. V. Neimark, *Langmuir*, 2000, **16**, 2419-2423.

723   (27) H. He, R. L. Frost, T. Bostrom, P. Yuan, L. Duong, D. Yang, Y. Xi and J. T.

724   Kloprogge, *Appl. Clay Sci.*, 2006, **31**, 262-271.

725   (28) H. He, Y. Ma, J. Zhu, P. Yuan and Y. Qing, *Appl. Clay Sci.*, 2010, **48**, 67-72.

726   (29) H. He, Q. Zhou, W. N. Martens, T. J. Kloprogge, P. Yuan, Y. Xi, J. Zhu and R. L.

727   Frost, *Clays Clay Miner.*, 2006, **54**, 689-696.

728   (30) H. He, D. Yang, P. Yuan, W. Shen and R. L. Frost, *J. Colloid Interface Sci.*, 2006, **297**,

729   235-243.

730   (31) J. H. Choy, S. Y. Kwak, Y. S. Han and B. W. Kim, *Mater. Lett.*, 1997, **33**, 143-147.

731   (32) G. Moussavi, A. Alahabadi, K. Yaghmaeian and M. Eskandari, *Chem. Eng. J.*, 2013,

732   **217**, 119-128.

733   (33) W. T. Jiang, P. H. Chang, Y. S. Wang, Y. Tsai, J. S. Jean, Z. Li and K. Krukowski, *J.*

734   *Hazard. Mater.*, 2013, **250-251**, 362-369.

735   (34) C. J. Wang, Z. Li, W. T. Jiang, J. S. Jean and C. C. Liu, *J. Hazard. Mater.*, 2010, **183**,

736   309-314.

737   (35) L. Zhu and R. Zhu, *Colloids Surf. A*, 2008, **320**, 19-24.

738   (36) T. Wang, J. Zhu, R. Zhu, F. Ge, P. Yuan and H. He, *J. Hazard. Mater.*, 2010, **178**,

739   1078-1084.

740   (37) R. Zhu, L. Zhu, J. Zhu and L. Xu, *Sep. Purif. Technol.*, 2008, **63**, 156-162.

741   (38) H. M. F. Freundlich, *Z. Phys. Chem.*, 1906, **57(A)**, 385-470.

742   (39) O. Hamdaoui, *J. Hazard. Mater.*, 2006, **135**, 264-273.

743   (40) I. Langmuir, *J. Am. Chem. Soc.*, 1918, **40**, 1361-1403.

744   (41) T. W. Weber and R. K. Chakravorti, *AiChE J.*, 1974, **20**, 228-238.

745   (42) C. H. Giles, T. H. MacEwan, S. N. Nakhwa and D. Smith, *J. Chem. Soc.*, 1960, **786**,

746   3973-3993.

747   (43) D. O. Cooney, *Clin. Toxicol.*, 1995, **33**, 213-217.

748   (44) R. Ding, P. Zhang, M. Seredych and T. J. Bandosz, *Water Res.*, 2012, **46**, 4081-4090.

749   (45) S. X. Zha, Y. Zhou, X. Jin and Z. Chen, *J. Environ. Manage.*, 2013, **129**, 569-576.

750   (46) W. S. Adriano, V. Veredas, C. C. Santana and L. R. B. Goncalves, *Biochem. Eng. J.*,

751   2005, **27**, 132-137.

752   (47) K. K. H. Choy, J. F. Porter and G. McKay, *J. Chem. Eng. Data*, 2000, **45**, 575-584.

753   (48) S. J. Allen, G. McKay and J. F. Porter, *J. Colloid Interface Sci.*, 2004, **280**, 322-333.

754   (49) S. Al-Asheh, F. Banat, R. Al-Omari and Z. Duvnjak, *Chemosphere*, 2000, **41**, 659-665.

755   (50) A. A. Khan and R. P. Singh, *Colloids Surf.*, 1987, **24**, 33-42.

756   (51) Q. Wu, Z. Li, H. Hong, R. Li and W. T. Jiang, *Water Res.*, 2013, **47**, 259-268.

757   (52) C. Gu and K. G. Karthikeyan, *Environ. Sci. Technol.*, 2005, **39**, 9166-9173.

758

759   **Table 1.** Molecular structure and some specific information about amoxicillin and ampicillin

	Amoxicillin	Ampicillin
Molecular structure		
Physical state	white to off-white solid	white to off-white solid
Molar mass (g/mol)	365.4	349.4
Chemical formula	$C_{16}H_{19}N_3O_5S$	$C_{16}H_{19}N_3O_4S$
Water solubility, 25 °C (g/L)	3.43	10.1
pK_a	2.4 (carboxylic)	2.7 (carboxylic)
	7.4 (amine)	7.3 (amine)
	9.6 (phenol)	
Environmental persistence data Photodegradation rate (s^{-1})		
Direct[†]	5.24×10^{-7}	not available
Hydrolysis rate (s^{-1})[‡]	4.45×10^{-7}	2.15×10^{-7}

760   [†] Direct photodegradation at pH 7 using a solar simulator system.

761   [‡] Hydrolysis at pH 7 and room temperature (298.15 K); the hydrolysis rate constants

762   correspond to half-lives of 18 d for amoxicillin and 36 d for ampicillin.

763

764

765 **Table 2.** Correlation isotherm parameters for adsorption of amoxicillin and ampicillin in

766 single component systems as fitted with Freundlich and Langmuir models

Adsorbent	Adsorbate	T (K)	Freundlich parameters			Langmuir parameters			
			K_F (mmol/g).(L/mmol)$^{-n}$	n	R^2	q_m (mmol/g)	K_L (L/mmol)	R^2	R_L
Na-MMT	Ampicillin	303.15	0.083	9.54	0.87	0.079	124.81	0.99	0.0092
		313.15	0.089	15.12	0.82	0.080	158.09	0.98	0.0073
		323.15	0.097	8.51	0.86	0.090	169.56	0.98	0.0068
	Amoxicillin	303.15	0.058	15.86	0.86	0.056	96.68	0.99	0.0124
		313.15	0.068	13.96	0.85	0.064	108.29	0.98	0.0111
		323.15	0.074	12.45	0.86	0.071	113.46	0.99	0.0106
O-MMT	Ampicillin	303.15	0.151	10.22	0.95	0.143	141.11	0.95	0.0082
		313.15	0.156	10.34	0.97	0.146	183.37	0.94	0.0063
		323.15	0.170	12.53	0.96	0.157	206.44	0.94	0.0056
	Amoxicillin	303.15	0.129	15.30	0.94	0.124	122.94	0.93	0.0098
		313.15	0.132	14.32	0.94	0.126	143.75	0.97	0.0084
		323.15	0.134	13.03	0.98	0.133	182.58	0.95	0.0066

767

768 **Table 3.** The fitted and calculated equilibrium parameters for binary adsorption of effluents

769 containing amoxicillin (adsorbate 1) and ampicillin (adsorbate 2)[*]

Effluents	Fitted Parameters		Calculated Parameters			R^2
	θ_1	θ_2	$K_{L,1(bin)}$ (L/mmol)	$K_{L,2(bin)}$ (L/mmol)	$q_{m,bin}$ (mmol/g)	
A	0.639	0.253	88.07	40.02	0.115	0.97
B	0.437	0.455	60.23	71.98	0.119	0.98
C	0.263	0.618	36.70	98.98	0.121	0.98

770 [*]Adsorption temperature = 303.15 K, Adsorbent = O-MMT

771

772 **Table 4.** Thermodynamic parameters for adsorption of amoxicillin and ampicillin in single

773 component systems

Adsorbents	T (K)	Amoxicillin			Ampicillin		
		$\Delta G°$ (kJ/mol)	$\Delta S°$ (J/mol.K)	$\Delta H°$ (kJ/mol)	$\Delta G°$ (kJ/mol)	$\Delta S°$ (J/mol.K)	$\Delta H°$ (kJ/mol)
Na-MMT	303.15	-5.55	162.8	43.8	-8.78	178.4	45.3
	313.15	-7.18			-10.56		
	323.15	-8.81			-12.35		
O-MMT	303.15	-9.92	191.4	48.1	-12.12	203.6	49.6
	313.15	-11.84			-14.16		
	323.15	-13.75			-16.19		

774
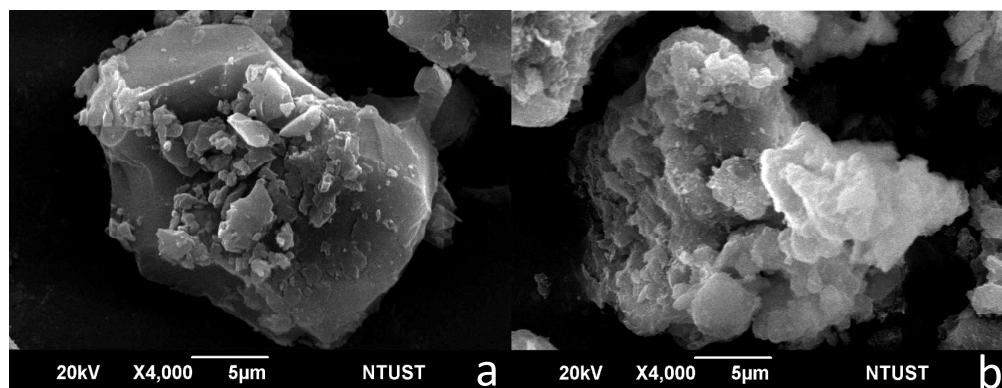
Figure 1. SEM images of Na-MMT (a) and O-MMT (b)
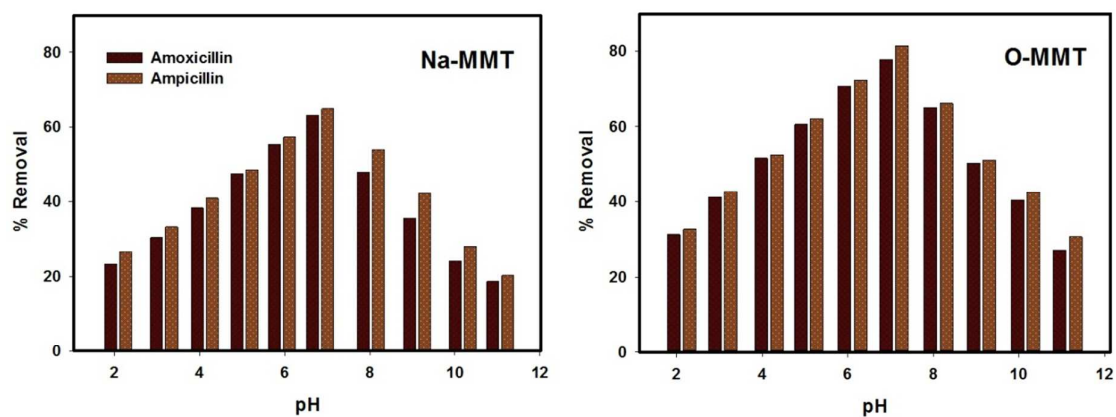
801

802 **Figure 2.** Variation of pHs on the removal of amoxicillin and ampicillin in single component
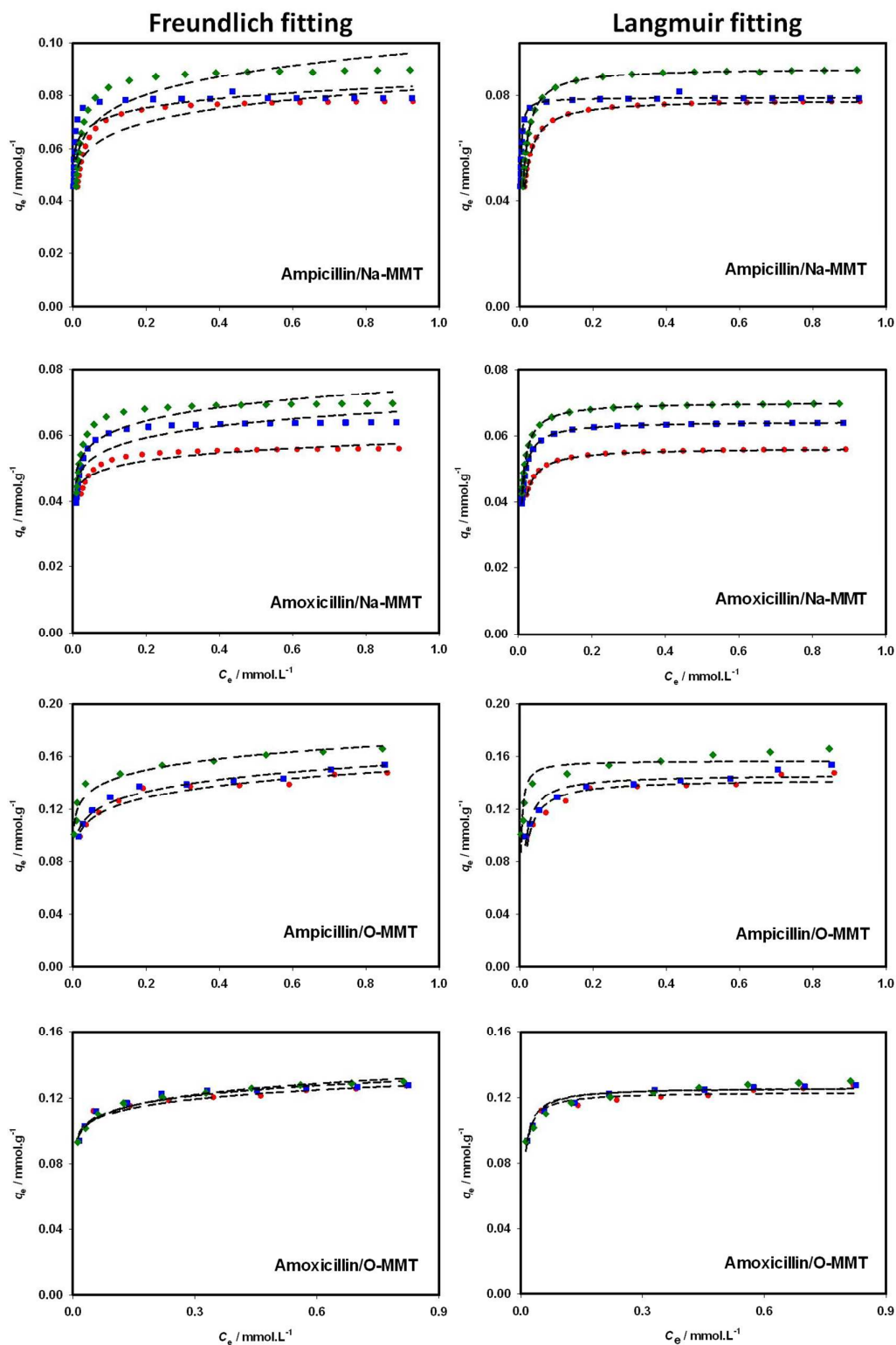
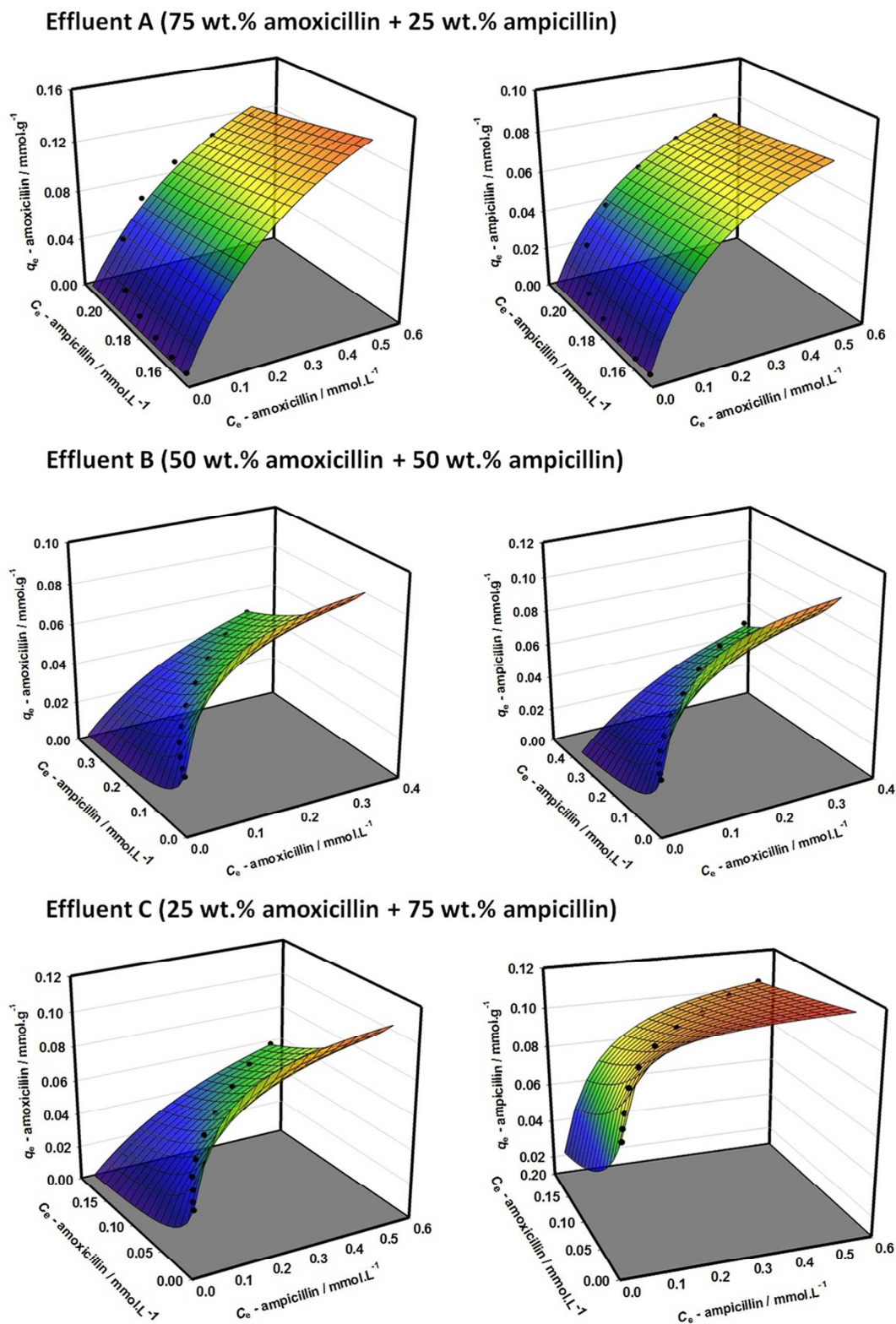803 systems (adsorbent dosage = 1 g/L, contact time = 24 h, T = 303.15 K)

804

805

806

807

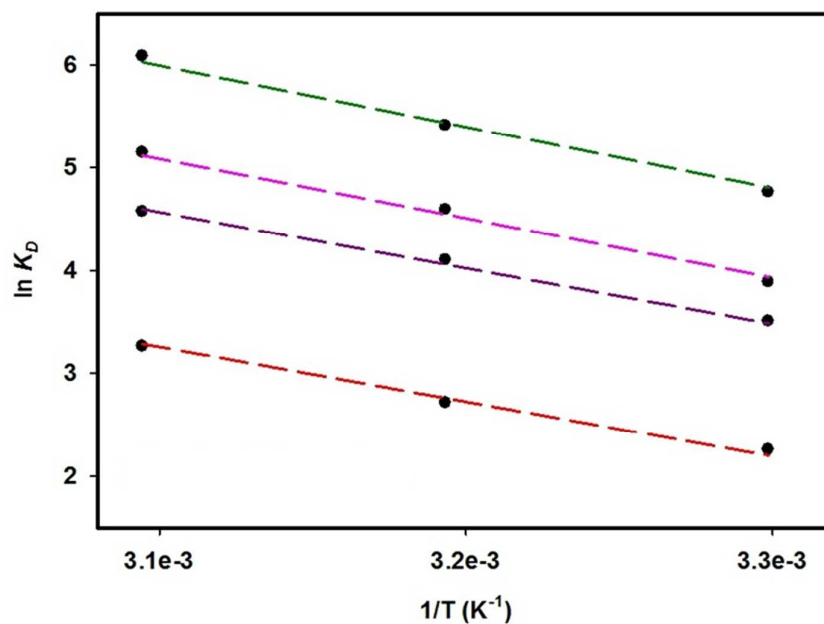**Figure 3.** The Freundlich and Langmuir model fittings against single adsorption equilibrium data of amoxicillin and ampicillin ($\bullet$ 303.15 K, $\blacksquare$ 313.15 K and $\blacklozenge$ 323.15 K)

808

809

810

Figure 4. The fitting performance of modified extended-Langmuir model against binary

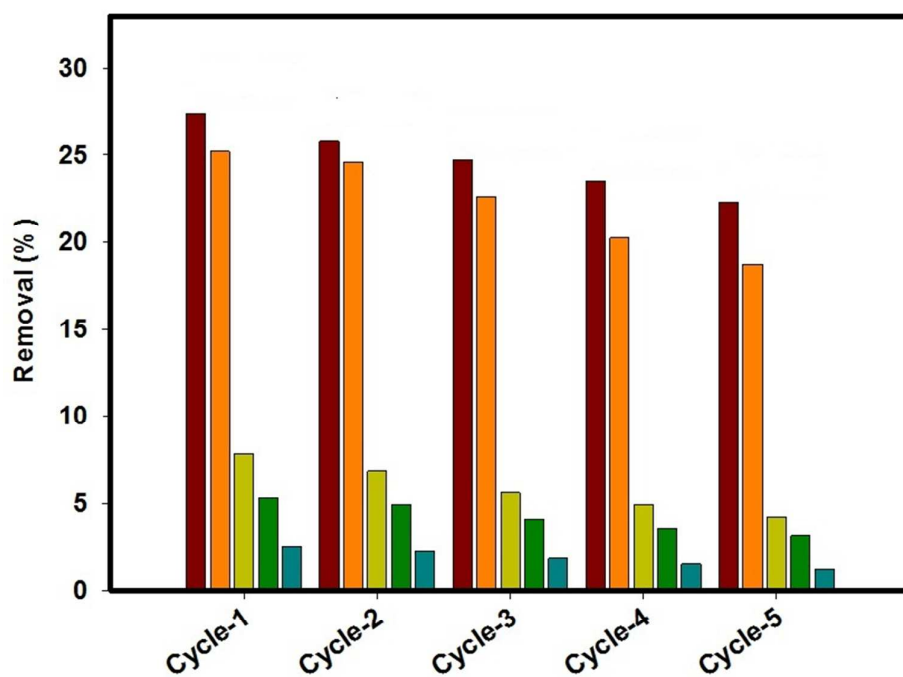adsorption equilibrium data of various effluents containing amoxicillin and ampicillin

38

814

815   **Figure 5**. Thermodynamic plots of ln K_D versus 1/T for the adsorption of amoxicillin and

816   ampicillin in single component systems (amoxicillin/Na-MMT;

817   ampicillin/Na-MMT;   amoxicillin/O-MMT;   ampicillin/O-MMT)

818

819

820

821 **Figure 6.** Removal percentages of various antibiotics in real pharmaceutical effluents and

822 reusability tests of O-MMT adsorbent

823 (■ amoxicillin; ■ ampicillin; ■ chloramphenicol; ■ ciprofloxacin; ■ cefotaxime)
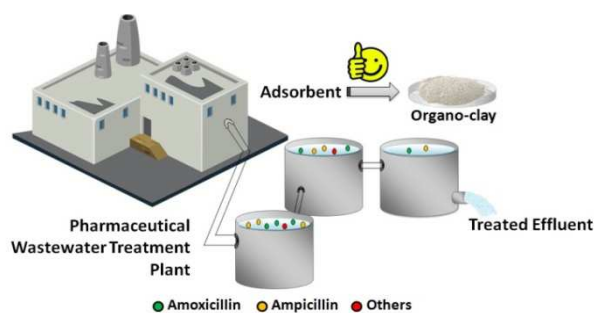
824

825

826

827

For Table of Contents Use Only

Antibiotics detoxification from synthetic and real effluents using a novel MTAB surfactant-montmorillonite (organoclay) sorbent

Merry Anggraini, Alfin Kurniawan, Lu Ki Ong, Mario A. Martin, Jhy-Chern Liu, Felycia E. Soetaredjo, Nani Indraswati, Suryadi Ismadji

A novel organoclay (MTAB surfactant-montmorillonite) sorbent showed its potential for the removal of amoxicillin and ampicillin antibiotics from synthetic and real effluents.